Conjugated Polymers

DOI: 10.1002/anie.201202570

# Color Tuning in Polymer Light-Emitting Diodes with Lewis Acids**

*Peter Zalar, Zachary B. Henson, Gregory C. Welch, Guillermo C. Bazan,* and Thuc-Quyen Nguyen**

Conjugated polymers possess electronically delocalized backbones, which lead to semiconducting behavior. Structural modifications afford a fine control over optical and electronic properties.[1] These methods have been exploited to tailor properties for a wide range of applications including polymer light-emitting diodes (PLEDs),[2] field-effect transistors,[3] photovoltaics,[4] and photodetectors.[5]

Molecular engineering strategies exist for tuning the optoelectronic properties of conjugated polymers. These include the choice of repeat unit, stabilization of the quinoidal resonance structure, planarization of repeat units, incorporation of main group elements, cross-conjugation, and the use of donor–acceptor alternating or statistical copolymers.[6] It is also possible to tune the optical properties of the bulk by using polymer/polymer, polymer/small molecule and polymer/phosphor blends.[7]

Addition of acids to conjugated polymers containing basic functionalities is yet another strategy for color modulation and redistribution of electron density.[8] More recently Lewis acids were used to influence the degree of charge-transfer character of narrow band gap polymers and oligomers.[9] This strategy allows control of optical properties through modulation of the Lewis acid strength. Additionally, since the adducts are formally zwitterionic, one avoids the presence of free mobile ions in the polymer matrix.[10]

Here we demonstrate the use of Lewis acid–base interactions to tune the properties of F8Py (see Scheme 1). Octyl side chains were chosen to improve the solubility. Incorporation of the pyridine co-monomer provides a lone pair of electrons for binding of Lewis acids. Trivalent group 13 compounds work well in this respect because of their empty $p_z$ orbital. $B(C_6F_5)_3$ was specifically chosen for its strong Lewis acidity, resistance to air and moisture, and stability towards B–C cleavage.[11] The formation of a F8Py-$B(C_6F_5)_3$ adduct leads to extended photoluminescence (PL) lifetimes and increased solid-state quantum yields. These properties allowed this strategy to be successfully demonstrated in PLEDs to modify the electroluminescence (EL) characteristics.

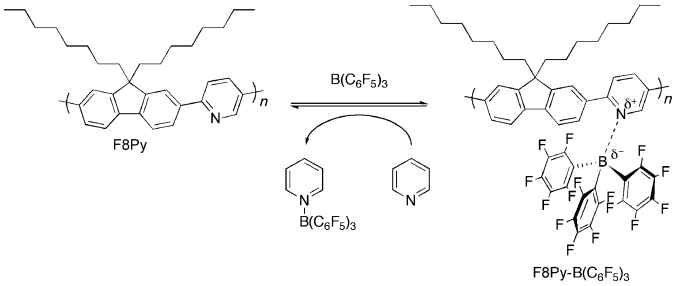


***Scheme 1.*** Reversible formation of an adduct between Lewis acidic B-$(C_6F_5)_3$ and Lewis basic F8Py in solution. Possible differences in the regiochemistry of Py units are not considered.[12]

UV/visible absorption and PL properties of various mixtures of the two components were used to examine F8Py-$B(C_6F_5)_3$ formation, see Figure 1. In dilute toluene solution (about $5 \times 10^{-6}$ M (in terms of repeat unit mass) or $2 \times 10^{-3}$ mg mL$^{-1}$), F8Py shows a broad absorption peak with

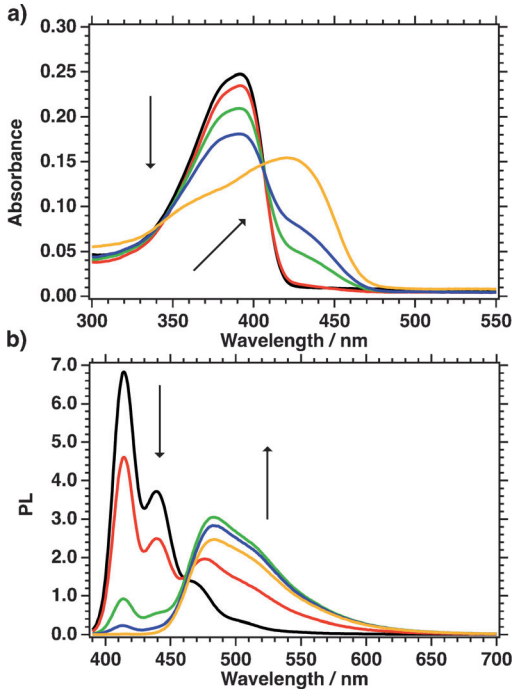


***Figure 1.*** a) UV/Vis absorption and b) PL spectra of F8Py in toluene after addition of 0.0 (black line), 0.1 (red line), 0.3 (green line), 0.7 (blue line), and 1.3 mol equivalents (orange line) $B(C_6F_5)_3$.

[*] P. Zalar, Z. B. Henson, Dr. G. C. Welch, Prof. Dr. G. C. Bazan, Prof. Dr. T.-Q. Nguyen
Center for Polymers and Organic Solids
University of California, Santa Barbara, CA 93106 (USA)
E-mail: bazan@chem.ucsb.edu
quyen@chem.ucsb.edu

[**] This work was supported by the DOE-BES (grant number DE-SC0002368), the NSF (grant number DMR 1005546), and the Camille Dreyfus Teacher-Scholar Award Program. T.-Q. N. is an Alfred P. Sloan Foundation Research Fellow. We are grateful to Dr. Alexander Mikhailovsky for assistance with the optical measurements and discussions. We thank Dr. Chunki Kim and Dr. Yuan Zhang for helpful discussions.

Supporting information for this article is available on the WWW under http://dx.doi.org/10.1002/anie.201202570.

a maximum ($\lambda_{max}$) of 392 nm and an onset ($\lambda_{onset}$) of 417 nm, in agreement with previous reports on structurally related polymers.[13] Incremental additions of $B(C_6F_5)_3$ gives rise to a reduction of the peak at 391 nm and the growth of a broad peak with $\lambda_{max} = 421$ nm and $\lambda_{onset} = 471$ nm (Figure 1a), resulting in a narrowing of the band gap. This change in absorption is consistent with F8Py-$B(C_6F_5)_3$ formation as shown in Scheme 1. Under these circumstances, $B(C_6F_5)_3$ withdraws electron density from the pyridine moiety leading to a lower energy charge-transfer band. Addition of pyridine regenerates the spectra of pristine F8Py because of the formation of the pyridine-$B(C_6F_5)_3$ adduct and liberation of the parent polymer, demonstrating that the binding is reversible.[14] The isosbestic point at 406 nm suggests that two separate species exist in solution, corresponding to $B(C_6F_5)_3$-bound and unbound polymer chains.

Figure 1b shows the PL spectra in toluene (excitation at 390 nm) upon addition of $B(C_6F_5)_3$ to F8Py. The PL spectrum of F8Py contains vibronic structure,[15] possessing distinct peaks at 414, 439, and 469 nm.[16] Stepwise addition of $B(C_6F_5)_3$ leads to a red shift in emission, resulting in an emission band spanning from 450 to 600 nm with $\lambda_{max} =$ 484 nm. Loss of vibronic fine structure has also been reported upon protonation of related polymers.[8] The quantum yields in solution do not change considerably (0.69–0.71) at all $B(C_6F_5)_3$ concentrations used in this study.

Figure 2 shows the solid-state absorption and PL spectra. The absorption of neat F8Py is red-shifted by 14 nm ($\lambda_{max}$ of 395 nm) relative to F8Py in solution. Successive addition of $B(C_6F_5)_3$ leads to a red-shift of $\lambda_{max}$ from 395 nm to 422 nm.

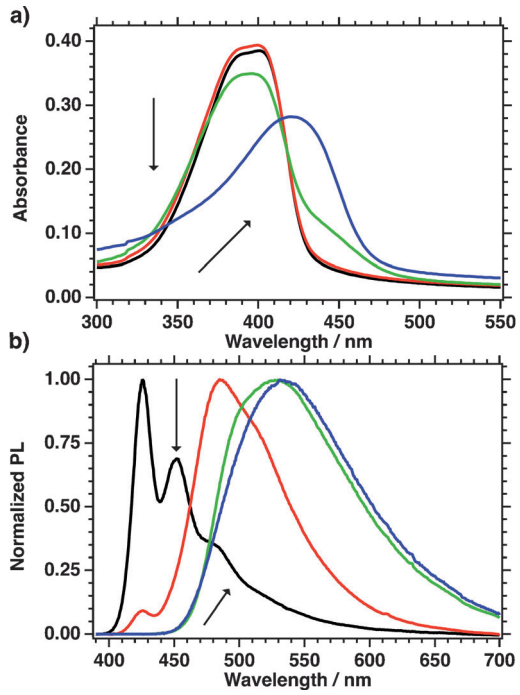


***Figure 2.*** a) UV/Vis absorption and b) PL spectra of F8Py and F8Py-$B(C_6F_5)_3$ adduct films containing 0.00 (black line), 0.01 (red line), 0.10 (green line), and 0.70 mol equivalents (blue line) $B(C_6F_5)_3$. The films were spin cast from toluene; the thickness is about 90 nm.

When compared to the spectra in solution, significant shifts are observed at lower concentrations of $B(C_6F_5)_3$ in the film because of a shift in the equilibrium towards adduct formation. The solid-state PL spectrum of neat F8Py contains vibronic fine structure with peaks at 424, 450, and 477 nm.[15,17] Adduct formation results in a broad PL band spanning from 450 to 700 nm. In contrast to the solution measurements, the film PL ceases to significantly evolve beyond the addition of 0.1 mol equivalents of $B(C_6F_5)_3$. These observations are consistent with interchain Förster resonance energy transfer (FRET) from free F8Py segments to F8Py-$B(C_6F_5)_3$ adduct sites. Furthermore, the PL quantum yield of adduct films increases from 0.20 for the parent polymer to 0.44 with 0.5 mol equivalents $B(C_6F_5)_3$, as measured using an integrating sphere.[18] We attribute this increase to less effective self-quenching because of the decreased planarity of the polymer chain upon binding of $B(C_6F_5)_3$ and the greater separation between chromophores as a result of the additional steric bulk.

PL lifetimes were investigated by time-correlated single-photon counting techniques to probe changes in the excited state dynamics. In the pristine F8Py solution, the emission at 440 nm is described by a monoexponential decay with a lifetime ($\tau$) of 444 ps. Upon addition of $B(C_6F_5)_3$, $\tau$ at 440 nm decays biexponentially with time constants of about 450 ps and about 50–70 ps, with the fast component contributing to up to 50% of the decay as more $B(C_6F_5)_3$ is added. The 50–70 ps component matches the width of our instrument response function, so the actual lifetimes may be shorter than the measured value. The emission at 480 nm, however, has a longer lived monoexponential decay with $\tau$ about 1.1 ns for any addition of $B(C_6F_5)_3$. A similar trend is observed in thin films, where $\tau$ at 480 nm for pristine F8Py is short lived (about 70 ps), while the PL decay of adduct films have multiexponential decays dominated by a time constant of about 2.1 ns. The longer $\tau$ of the F8Py-$B(C_6F_5)_3$ adducts can be explained by considering the formation of a new emissive state with a lower oscillator strength.[19]

The surface topology of F8Py and a film cast from a solution of F8Py containing 0.1 mol equivalents $B(C_6F_5)_3$ were examined by using atomic force microscopy (AFM, see the Supporting Information). Both films are smooth and lack any evidence of local order. The root mean square (rms) surface roughness values are nearly identical at 0.56 nm for pristine F8Py and 0.54 nm for F8Py-$B(C_6F_5)_3$.

Ultraviolet photoelectron spectroscopy (UPS) was used to determine the highest occupied molecular orbital (HOMO) energy levels of the F8Py and F8Py-$B(C_6F_5)_3$ (see the Supporting Information).[20] These results are summarized in Table 1. Upon addition of $B(C_6F_5)_3$, the HOMO level is stabilized.[9] However, the lowest unoccupied molecular orbital (LUMO) level is reduced to a greater extent, resulting in a decreased band gap.

The properties of F8Py-$B(C_6F_5)_3$ adducts seemed appropriate for incorporation into PLED devices as the emissive layer. The device structure consisted of indium–tin oxide (ITO)/poly(3,4-ethylene-dioxythiophene):poly(4-styrene sulphonic acid) (PEDOT:PSS)/poly(9-vinylcarbazole) (PVK)/F8Py + $X$ mol equivalents $B(C_6F_5)_3$/Ba/Al. PVK was included

***Table 1:*** Summary of EL emission maxima, CIE 1931 color space coordinates, turn-on voltages ($V_{on}$), HOMO levels for films (as determined by UPS), luminance efficiency (LE), and external quantum efficiency ($\eta_{ext}$) for devices containing specified molar equivalents of $B(C_6F_5)_3$.

| Molar equiv of $B(C_6F_5)_3$[a] | EL $\lambda_{max}$ [nm] | CIE $(x,y)$ | $V_{on}$ [V] | HOMO [eV] | LE [cd A$^{-1}$][b] | $\eta_{ext}$ [%][b] |
|---|---|---|---|---|---|---|
| 0.00 | 426 | (0.19,0.19) | 6.1 | −5.74 | 0.046 | 0.070 |
| 0.01 | 485 | (0.20,0.34) | 7.0 | −5.86 | 0.071 | 0.072 |
| 0.02 | 493 | (0.20,0.43) | 7.9 | −5.92 | 0.089 | 0.076 |

[a] Molar equivalents with respect to the approximate number of monomer units in solution. [b] At about 111 mA cm$^{-2}$.

as a hole-injecting/electron-blocking layer. Devices were fabricated in which 0.00, 0.01, and 0.02 mol equivalents $B(C_6F_5)_3$ were added. The resulting data are presented in Table 1 and representative EL spectra (obtained at a current density of 111 mA cm$^{-2}$) appear in Figure 3. As increasing amounts of $B(C_6F_5)_3$ are added to the film, the EL characteristics gradually red-shift. Gradual "quenching" of the F8Py emission takes place with growth of the F8Py-$B(C_6F_5)_3$ peak. At 0.02 equivalents $B(C_6F_5)_3$ the EL from the F8Py is weak, contributing less than 7% to the total EL. Since the $M_n$ of the polymer is about 25 kDa, this corresponds to approximately one $B(C_6F_5)_3$ molecule per polymer chain. Additions of $B(C_6F_5)_3$ beyond 0.02 mol equivalents lead to slightly more red-shifted EL, up to a $\lambda_{max}$ of 535 nm.

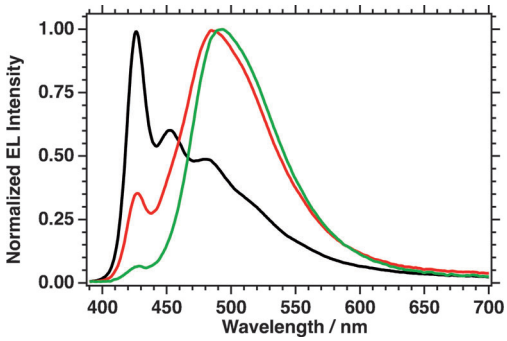


***Figure 3.*** EL spectra of F8Py at a constant current density of 111 mA cm$^{-2}$ for 0.00 (black line), 0.01 (red line), and 0.02 mol equivalents (green) $B(C_6F_5)_3$.

Complementary current density–voltage ($J$-$V$) and luminance–voltage ($L$–$V$) device characteristics are shown in Figure 4. Luminance efficiency–current density ($LE$–$J$) plots are provided in the Supporting Information. With more $B(C_6F_5)_3$, the $J$–$V$ and $L$–$V$ characteristics shift to higher biases, resulting in larger $V_{on}$ relative to the F8Py device (Figure 4). The shift of $J$–$V$ and $L$–$V$ towards higher biases could be due to a modification of injection barrier.[21] The $LE$–$J$ characteristics of each device are similar, with all luminance efficiencies residing within the same order of magnitude. Despite the increase in the operating voltage, the external quantum efficiency ($\eta_{ext}$) remains at about 0.07% until the addition of more than 0.02 mol equivalents $B(C_6F_5)_3$, where a reduction in $\eta_{ext}$ is observed (see the Supporting Information).

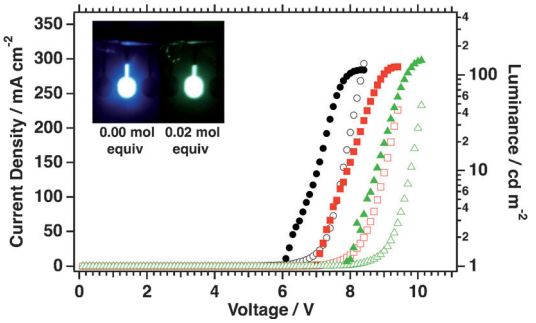


***Figure 4.*** Current density–voltage (open symbols; $J$-$V$) and luminance–voltage (closed symbols; $L$-$V$) plots for devices containing 0.00 (black circles), 0.01 (red squares), and 0.02 mol equivalents (green triangles) $B(C_6F_5)_3$.

The sequential vacuum level shift observed by UPS agrees with the trends observed for $V_{on}$ in the $J$–$V$ and $L$–$V$ plots. Since the HOMO of PVK is about −5.4 eV[22] and assuming no interfacial effects, the hole-injection barrier is increased from about 0.3 eV to about 0.6 eV.[23] Considering that the HOMO and LUMO energy levels are lowered for F8Py-$B(C_6F_5)_3$, the hole-injection barrier is increased while the electron-injection barrier (if using a low work function cathode, such as Ba) remains unaffected. However, it is worth pointing out that adduct formation at the concentrations studied here does not adversely affect the luminance efficiency or external quantum efficiency, while allowing for tuning of the emissive properties.

In conclusion, mixing of a Lewis basic polymer with a Lewis acid allows the absorption and PL properties to be modified in a simple chemical step. The solutions and films containing F8Py-$B(C_6F_5)_3$ adducts exhibit longer excited state lifetimes and larger quantum yields than the native F8Py. PLEDs were also successfully fabricated using F8Py and F8Py-$B(C_6F_5)_3$ adducts as the emissive layer. The EL spectra shift to longer wavelengths as the fraction of polymer bound to $B(C_6F_5)_3$ is increased. When 0.10 monomer equivalents of $B(C_6F_5)_3$ is added, the emission of the pristine polymer at 426 nm is completely suppressed, resulting in an EL with a $\lambda_{max}$ of 509 nm. The $LE$–$J$ characteristics were not significantly influenced by F8Py-$B(C_6F_5)_3$ formation, however, $J$–$V$ and $L$–$V$ characteristics shifted to higher voltages. These shifts can be readily rationalized in the context of larger hole-injection barriers as the HOMO level of the semiconducting film decreases with increasing [F8Py-$B(C_6F_5)_3$]. The use of alternative hole-injection electrodes is anticipated to circumvent this feature. Lewis acid–base interactions therefore provide a straightforward way to modulate optoelectronic properties in PLEDs without influence on the device external quantum efficiency. This strategy should readily be adapted to other organic electronic applications in which fine-tuning of energy levels is important for the operation and performance of the device.

Received: April 2, 2012
Revised: May 5, 2012
Published online: June 5, 2012

  

**Keywords:** boron · Lewis acids · light-emitting diodes · luminescence · polymers

[1] a) S. R. Forrest, M. E. Thompson, *Chem. Rev.* **2007**, *107*, 923 – 925; b) G. Hadziioannou, P. F. van Hutten, *Semiconducting Polymers: Chemistry, Physics and Engineering*, Wiley-VCH, Weinheim, **2000**; c) F. So, *Organic Electronics: Materials, Processing, Devices and Applications*, CRC, Boca Raton, **2010**; d) H. Klauk, *Organic Materials: Materials, Manufacturing and Applications*, Wiley-VCH, Weinheim, **2006**.

[2] a) A. C. Grimsdale, K. L. Chan, R. E. Martin, P. G. Jokisz, A. B. Holmes, *Chem. Rev.* **2009**, *109*, 897 – 1091; b) P. M. Beaujuge, C. M. Amb, J. R. Reynolds, *Acc. Chem. Res.* **2010**, *43*, 1396 – 1407; c) C. M. Amb, A. L. Dyer, J. R. Reynolds, *Chem. Mater.* **2011**, *23*, 397 – 415.

[3] A. R. Murphy, J. M. J. Fréchet, *Chem. Rev.* **2007**, *107*, 1066 – 1096.

[4] a) P.-L. T. Boudreault, A. Najari, M. LeClerc, *Chem. Mater.* **2011**, *23*, 456 – 469; b) Y.-J. Cheng, S.-H. Yang, C.-S. Hsu, *Chem. Rev.* **2009**, *109*, 5868 – 5923; c) J. Chen, Y. Cao, *Acc. Chem. Res.* **2009**, *42*, 1709 – 1718.

[5] X. Gong, M. Tong, Y. Xia, W. Cai, J. S. Moon, Y. Cao, G. Yu, C. L. Shieh, B. Nilsson, A. J. Heeger, *Science* **2009**, *325*, 1665.

[6] a) A. Kraft, A. C. Grimsdale, A. B. Holmes, *Angew. Chem.* **1998**, *110*, 416 – 443; *Angew. Chem. Int. Ed.* **1998**, *37*, 402 – 428; b) U. Scherf, E. J. W. List, *Adv. Mater.* **2002**, *14*, 477 – 487; c) J. Roncali, *Chem. Rev.* **1997**, *97*, 173 – 205; d) A. C. Grimsdale, K. L. Chan, R. E. Martin, P. G. Jokisz, A. B. Holmes, *Chem. Rev.* **2009**, *109*, 897 – 1091.

[7] a) M. Berggren, O. Inganäs, G. Gustafsson, J. Rasmusson, M. R. Andersson, T. Hjertberg, O. Wennerström, *Nature* **1994**, *372*, 444 – 446; b) Y. Kawamura, S. Yanagida, S. R. Forrest, *J. Appl. Phys.* **2002**, *92*, 87 – 93; c) X. Gong, M. R. Robinson, J. C. Ostrowski, D. Moses, G. C. Bazan, A. J. Heeger, *Adv. Mater.* **2002**, *14*, 581 – 585; d) M. Granström, O. Inganäs, *Appl. Phys. Lett.* **1996**, *68*, 116129 – 116131.

[8] a) S. Kappaun, S. Horner, A.-M. Kelterer, K. Waich, F. Grasse, M. Graf, L. Romaner, F. Niedermair, K. Müllen, A. C. Grimsdale, R. Saf, E. J. W. List, E. Zojer, C. Slugovc, *Macromol. Chem. Phys.* **2008**, *209*, 2122 – 2134; b) A. P. Monkman, L.-O. Pålsson, R. W. T. Higgins, C.-S. Wang, M. R. Bryce, A. S. Batsanov, J. A. K. Howard, *J. Am. Chem. Soc.* **2002**, *124*, 6049 – 6055; c) J. M. Hancock, S. A. Jenekhe, *Macromolecules* **2008**, *41*, 6864 – 6867; d) A. P. Monkman, M. Halim, I. D. W. Samuel, L. E. Horsburgh, *J. Chem. Phys.* **1998**, *109*, 10372 – 10378.

[9] a) G. C. Welch, R. Coffin, J. Peet, G. C. Bazan, *J. Am. Chem. Soc.* **2009**, *131*, 10802 – 10803; b) G. C. Welch, G. C. Bazan, *J. Am. Chem. Soc.* **2011**, *133*, 4632 – 4644; c) S. Hayashi, A. Asano, T. Koizumi, *Polym. Chem.* **2011**, *2*, 2764 – 2766.

[10] a) D. B. A. Rep, A. F. Morpurgo, W. G. Sloof, T. M. Klapwijk, *J. Appl. Phys.* **2003**, *93*, 2082 – 2090; b) J. C. deMello, N. Tessler, S. C. Graham, R. H. Friend, *Phys. Rev. B* **1998**, *57*, 12951 – 12963.

[11] a) W. E. Piers, *Adv. Organomet. Chem.* **2005**, *52*, 1 – 76; b) G. Erker, *Dalton Trans.* **2005**, 1883 – 1890; c) W. E. Piers, T. Chivers, *Chem. Soc. Rev.* **1997**, *26*, 345 – 354.

[12] L. Ying, B. B. Y. Hsu, H. M. Zhan, G. C. Welch, P. Zalar, L. A. Perez, E. J. Kramer, T.-Q. Nguyen, A. J. Heeger, W.-Y. Wong, G. C. Bazan, *J. Am. Chem. Soc.* **2011**, *133*, 18538 – 18541.

[13] a) B. Liu, W.-L. Yu, Y.-H. Lai, W. Huang, *Chem. Mater.* **2001**, *13*, 1984 – 1991; b) S.-P. Liu, S.-C. Ng, H. S. O. Chan, *Synth. Met.* **2005**, *149*, 1 – 11.

[14] A. G. Massey, A. J. Park, *J. Organomet. Chem.* **1966**, *5*, 218.

[15] a) C. Rothe, F. Galbrecht, U. Scherf, A. Monkman, *Adv. Mater.* **2006**, *18*, 2137 – 2140; b) M. J. Winokur, J. Slinker, D. L. Huber, *Phys. Rev. B* **2003**, *67*, 184106; c) A. J. Cadby, P. A. Lane, H. Mellor, S. J. Martin, M. Grell, C. Giebeler, D. D. C. Bradley, M. Wohlgenannt, C. An, Z. V. Vardeny, *Phys. Rev. B* **2000**, *62*, 15604 – 15609.

[16] A. L. T. Khan, P. Sreearunothai, L. M. Herz, M. J. Banach, A. Köhler, *Phys. Rev. B* **2004**, *69*, 0852011 – 0852018.

[17] a) U. Scherf, E. J. W. List, *Adv. Mater.* **2002**, *14*, 477 – 487; b) Q.-B. Pei, Y. Yang, *J. Am. Chem. Soc.* **1996**, *118*, 7416 – 7417; c) M. Leclerc, *J. Polym. Sci. Part A* **2001**, *39*, 2867 – 2873.

[18] N. C. Greenham, I. D. W. Samuel, G. R. Hayes, R. T. Phillips, Y. Kessener, S. C. Moratti, A. B. Holmes, R. H. Friend, *Chem. Phys. Lett.* **1995**, *241*, 89 – 96.

[19] a) C. Dehu, F. Meyers, J. L. Brédas, *J. Am. Chem. Soc.* **1993**, *115*, 6198 – 6206; b) J. Cornil, D. A. dos Santos, D. Beljonne, J. L. Brédas, *J. Phys. Chem.* **1995**, *99*, 5604 – 5611; c) B. Henderson, G. Imbusch, *Optical Spectroscopy of Inorganic Solids*, Oxford University Press, Oxford, **1989**.

[20] H. Ishii, K. Sugiyama, E. Ito, K. Seki, *Adv. Mater.* **1999**, *11*, 605 – 625.

[21] a) I. D. Parker, *J. Appl. Phys.* **1994**, *75*, 1656 – 1666; b) I. H. Campbell, J. D. Kress, R. L. Martin, D. L. Smith, N. N. Barashkov, J. P. Ferrais, *Appl. Phys. Lett.* **1997**, *71*, 3528 – 3530; c) B. de Boer, A. Hadipour, M. M. Mandoc, T. van Woudenbergh, P. W. M. Blom, *Adv. Mater.* **2005**, *17*, 621 – 625.

[22] X. Gong, J. C. Ostrowski, D. Moses, G. C. Bazan, A. J. Heeger, *Adv. Funct. Mater.* **2003**, *13*, 439 – 444.

[23] *Organic Electroluminescent Materials and Devices*; (Ed.: S. Miyata), Gordon & Breach, New York, **1997**, pp. 218 – 234.

  